Thermomechanical Properties of Poly(methyl methacrylates) containing Tethered and Untethered Polyhedral Oligomeric Silsesquioxanes (POSS)

Edward T. Kopesky[1], Timothy S. Haddad[2], Robert E. Cohen[1], Gareth H. McKinley[3]*

[1]Department of Chemical Engineering, Massachusetts Institute of Technology, [2]ERC Inc., Air Force Research Laboratory, Edwards AFB, CA 93524, [3]Department of Mechanical Engineering, Massachusetts Institute of Technology

Abstract

Poly(methyl methacrylates) (PMMA) containing both tethered and untethered polyhedral oligomeric silsesquioxanes (POSS) were investigated using wide angle X-ray diffraction (WAXD), differential scanning calorimetry (DSC), and rheological characterization.
Unfilled, entangled polymers were synthesized and tested in small amplitude oscillatory shear. The addition of tethered-POSS to the PMMA chain leads to a decrease in the plateau modulus (G_N^0) as expected from previous results on POSS-polymer rheology. Cyclohexyl-POSS and isobutyl-POSS were blended with PMMA homopolymer, and isobutyl-POSS was also blended with a POSS-PMMA copolymer containing 25 wt% tethered isobutyl-POSS distributed randomly along the chain. Both DSC and rheological results suggest a regime at low untethered-POSS loadings (≤ 5 vol%) in PMMA in which much of the POSS filler resides in the matrix in a nanoscopically-dispersed state. This well-dispersed POSS acts as a plasticizer and leads to a decrease in the zero-shear-rate viscosity (η_0) at low loadings. Above this regime, an apparent solubility limit is reached at which point additional untethered-POSS aggregates into crystallites in the PMMA matrix and both the viscosity and the plateau modulus increase in a way consistent with classical predicitions for hard-sphere-filled suspensions. The principles of time-temperature superposition are followed by these nanocomposites; however, fits to the WLF equation show no strong trend with increasing POSS loading and therefore could not explain the decrease in viscosity in light of an increase in free volume. Blends of untethered-POSS with copolymer show a significant increase in η_0 for all loadings, greater than that expected for traditional hard-

Distribution A. Approved for public release, distribution unlimited.

Report Documentation Page

Form Approved
OMB No. 0704-0188

Public reporting burden for the collection of information is estimated to average 1 hour per response, including the time for reviewing instructions, searching existing data sources, gathering and maintaining the data needed, and completing and reviewing the collection of information. Send comments regarding this burden estimate or any other aspect of this collection of information, including suggestions for reducing this burden, to Washington Headquarters Services, Directorate for Information Operations and Reports, 1215 Jefferson Davis Highway, Suite 1204, Arlington VA 22202-4302. Respondents should be aware that notwithstanding any other provision of law, no person shall be subject to a penalty for failing to comply with a collection of information if it does not display a currently valid OMB control number.

1. REPORT DATE **27 MAY 2004**	2. REPORT TYPE	3. DATES COVERED **-**
4. TITLE AND SUBTITLE **Thermomechanical Properties of Poly (methyl methacrylates) Containing Tethered and Untethered Polyhedral Oligomeric Silsesquioxanes (POSS)**		5a. CONTRACT NUMBER **F04611-99-C-0025** 5b. GRANT NUMBER 5c. PROGRAM ELEMENT NUMBER
6. AUTHOR(S) **Edward Kopesky; Timothy Haddad; Robert Cohen; Gareth McKinley**		5d. PROJECT NUMBER **2303** 5e. TASK NUMBER **M1A3** 5f. WORK UNIT NUMBER **2303M1A3**
7. PERFORMING ORGANIZATION NAME(S) AND ADDRESS(ES) **ERC INCORPORATED,555 Sparkman Drive,Huntsville,AL,35816-0000**		8. PERFORMING ORGANIZATION REPORT NUMBER
9. SPONSORING/MONITORING AGENCY NAME(S) AND ADDRESS(ES)		10. SPONSOR/MONITOR'S ACRONYM(S) 11. SPONSOR/MONITOR'S REPORT NUMBER(S)
12. DISTRIBUTION/AVAILABILITY STATEMENT **Approved for public release; distribution unlimited**		
13. SUPPLEMENTARY NOTES		

14. ABSTRACT

Poly(methyl methacrylates) (PMMA) containing both tethered and untethered polyhedral oligomeric silsesquioxanes (POSS) were investigated using wide angle X-ray diffraction (WAXD), differential scanning calorimetry (DSC), and rheological characterization. Unfilled, entangled polymers were synthesized and tested in small amplitude oscillatory shear. The addition of tethered-POSS to the PMMA chain leads to a decrease in the plateau modulus (GN0) as expected from previous results on POSS-polymer rheology. Cyclohexyl-POSS and isobutyl-POSS were blended with PMMA homopolymer, and isobutyl-POSS was also blended with a POSS-PMMA copolymer containing 25 wt% tethered isobutyl-POSS distributed randomly along the chain. Both DSC and rheological results suggest a regime at low untethered-POSS loadings (¡Ü 5 vol%) in PMMA in which much of the POSS filler resides in the matrix in a nanoscopically-dispersed state. This well-dispersed POSS acts as a plasticizer and leads to a decrease in the zero-shear-rate viscosity (¦Ç0) at low loadings. Above this regime, an apparent solubility limit is reached at which point additional untethered-POSS aggregates into crystallites in the PMMA matrix and both the viscosity and the plateau modulus increase in a way consistent with classical predicitions for hard-sphere-filled suspensions. The principles of time-temperature superposition are followed by these nanocomposites; however, fits to the WLF equation show no strong trend with increasing POSS loading and therefore could not explain the decrease in viscosity in light of an increase in free volume. Blends of untethered-POSS with copolymer show a significant increase in ¦Ç0 for all loadings, greater than that expected for traditional hard-sphere fillers. This is a result of associations between untethered-POSS and tethered-POSS cages in the blend, which retard chain relaxation processes in a way not seen in either the homopolymer blends or the unfilled copolymers. Time-temperature superposition also holds for the filled copolymers and these blends show a strong increase increase in the WLF coefficients, suggesting that both free volume and viscosity increase with filler loading.

15. SUBJECT TERMS

16. SECURITY CLASSIFICATION OF:			17. LIMITATION OF ABSTRACT	18. NUMBER OF PAGES	19a. NAME OF RESPONSIBLE PERSON
a. REPORT	b. ABSTRACT	c. THIS PAGE			
unclassified	**unclassified**	**unclassified**		**42**	

sphere fillers. This is a result of associations between untethered-POSS and tethered-POSS cages in the blend, which retard chain relaxation processes in a way not seen in either the homopolymer blends or the unfilled copolymers. Time-temperature superposition also holds for the filled copolymers and these blends show a strong increase increase in the WLF coefficients, suggesting that both free volume and viscosity increase with filler loading.

Introduction

Polyhedral oligomeric silsesquioxanes (POSS)[1] have drawn considerable interest due to their hybrid organic-inorganic structure which consists of a silica cage with organic R-groups on the corners.[2-5] A generic POSS molecule ($R_8Si_8O_{12}$) is shown at the top of Figure 1. When covalently tethered to a polymer backbone, POSS has been shown to improve the thermo-oxidative stabilities of polymers,[6] increase their glass transition temperatures,[7-9] lower their zero-shear-rate viscosities,[10] and increase the toughness of homopolymer blends.[11] POSS may be incorporated into a polymer matrix in two primary ways: chemically tethered to the polymer or as untethered filler particles, both of which are shown in Figure 1. (For brevity we will at times denote these limits as CP and F, respectively, to denote POSS copolymer and POSS filler.) In the copolymer case, one corner of the POSS macromer is functionalized, allowing it to be grafted onto the polymer backbone. Untethered POSS filler differs in that all corners of the cages have the same R-group and are non-reactive. The edges of the ternary composition diagram shown in Figure 1 indicate that there are three types of binary blends to consider: untethered POSS may be blended with either the homopolymer, poly(methyl methacrylate) (PMMA) in this case, or with a tethered-POSS-containing copolymer, which in this study has a PMMA backbone. The homopolymer and the copolymer may also be blended together. The interior of the triangular diagram represents the variety of ternary compositions that can be formulated. The present study focuses exclusively on the filler-homopolymer (F/HP) and the filler-copolymer (F/CP) sides of the composition space in order to discern systematic differences, both quantitative and qualitative, between the thermomechanical properties of these two binary blend systems. The range of compositions studied are indicated by the two arrows in Fig. 1.

A key factor in optimizing the properties of a POSS-polymer system is the thermodynamic interaction between the pendant R-group and the matrix. This controls the degree of dispersion of POSS in the matrix and thus the degree of property enhancement. Untethered POSS particles can disperse on a molecular scale (~1.5 nm) or as crystalline

aggregates which can be on the order of microns in size.[12] An important question is whether both of these states exist simultaneously, and to varying degrees, in a given POSS-polymer blend. Additional morphologies are possible when tethered-POSS particles are present. Their covalent attachment to the polymer backbone limits the length scale of association and has been shown to lead to two-dimensional raft-like structures[13] which are shaped similarly to clay platelets.[14]

Rheological characterization is an important tool for comparing behavior of the F/HP and the F/CP blend systems. Previous work on POSS rheology has been scarce, with few relevant publications.[10,15] In a study by Romo-Uribe et al.(1998),[10] poly(methyl styrenes) containing two different types of tethered-POSS [R = cyclopentyl (0-63 wt%) and R = cyclohexyl (0-64 wt%] were tested in small amplitude oscillatory shear flow. One notable result was the appearance of a rubbery plateau (~10^3 Pa) in the storage modulus G' at low frequencies in the 45wt% cyclopentyl-POSS copolymer, suggesting formation of a percolated network by the tethered-POSS particles. Low frequency plateaus in G' were not observed for 28 wt% cyclopentyl-POSS and 27 wt% cyclohexyl-POSS. Zero-shear-rate viscosities were reported for the polymers exhibiting conventional terminal flow behavior. For a 42 wt% cyclohexyl-POSS copolymer of molecular weight M_w = 120,000 g/mol and degree of polymerization x_w = 420, the viscosity was approximately half that of the homopolymer, which had M_w and x_w values of only 34,000 g/mol and 180, respectively. The study of Romo-Uribe et al. used only unentangled to very mildly entangled polymers, so no detailed information on plateau moduli and hence entanglement molecular weight (M_e) could be obtained.

The rheological properties of blends of homopolymers and untethered-POSS were investigated by Fu et al.(2003)[15] for ethylene-propylene copolymer containing 0, 10, 20 and 30 wt% methyl-POSS. At high frequencies, for loadings up to 20 wt%, the storage modulus G' remained essentially unchanged, only diverging at low frequencies, where a plateau of increasing magnitude (10^2 – 10^3 Pa) formed at high POSS loadings. This plateau was attributed to the presence of POSS crystals in the matrix, which were observed in wide angle X-ray diffraction. Viscometric tests showed that the viscosity of the unfilled polymer and the 10wt%-filled blend were essentially unchanged over a shear rate range of 10^{-4} – 10^{-1} s^{-1}, while the viscosities of the 20 wt% and 30 wt% blends were substantially higher over the same shear rate range. No information on rheological behavior at loadings below 10 wt% was reported.

Studies of other (non-POSS) nanoparticles have demonstrated the unusual effect very small (~ 10 nm) nanoparticles have on polymer matrices.[16,17] In the work of Zhang and Archer (2002),[16] poly(ethylene oxide) was filled with two types of 12 nm silica particles. In one case, the particles received no surface treatment, allowing them to hydrogen bond with the polymer matrix. Predictably, a dramatic enhancement in the linear viscoelastic properties was seen at very small loadings, with a low frequency plateau in the storage modulus G' appearing at a very small volume loading of particles $\phi \approx 2\%$. This was attributed to a substantial adsorbed layer of PEO on the particle surfaces and to particle agglomeration, the combination of which led to a substantially higher effective volume fraction, ϕ_e. However, when the particles were treated with a PEO-like organosilane there was virtually no difference between the linear viscoelastic properties of the PEO and a 2 vol% blend. In fact, the loss moduli G'' were virtually indistinguishable between the two samples in the terminal flow region, giving identical zero-shear-rate viscosities η_0 from linear viscoelasticity theory. This result suggests that polymers filled with very small nanoparticles (d~10 nm) with weak polymer-filler interactions do not follow the classical theory for hard-sphere-filled suspensions:[18]

$$\eta_0(\phi) = \eta_0(0)(1 + 2.5\phi + ...) \qquad (1)$$

which predicts a monotonic increase in viscosity with particle loading. This deviation from the classical result was further demonstrated by Mackay et al. (2003),[17] who filled linear polystyrene melts with highly crosslinked 5 nm polystyrene nanoparticles. A substantial decrease in viscosity – more than 50% for some compositions – was reported, but no consistent trend in viscosity with increasing particle loading was found. The drop in viscosity was attributed to an increase in free volume and a change in conformation of the polystyrene chains in the matrix, although neither of these causes was clearly demonstrated.

The present study seeks to determine if nanofilled polymer systems containing untethered POSS filler and tethered-POSS groups demonstrate similar unusual flow phenomena. The POSS nanoparticle-matrix interaction is different from those mentioned above in that there is the potential for molecularly dispersed nanoparticles, crystalline filler aggregates, and, in the tethered case, nanoscopic POSS domains which may form two-dimensional raft-like crystallites. The combined effect of these phases is addressed in the present study.

Experimental Section

Materials. The POSS $(R)_7Si_8O_{12}$(propyl methacrylate) monomers, R = isobutyl and cyclopentyl, were either synthesized according to the literature procedures[19] or obtained from Hybrid Plastics. Toluene (Fischer) was dried by passage through an anhydrous alumina column, vacuum transferred and freeze-pump-thawed three times prior to use. Methyl methacrylate (Aldrich) was passed through an inhibitor-removal column (Aldrich), freeze-pump-thawed twice, vacuum transferred to a collection vessel and stored at -25 ˚C in a glovebox under nitrogen. AIBN free radical initiator (TCI) was used as received. NMR spectra were obtained on a Bruker 400 MHz spectrometer and referenced to internal chloroform solvent (^{1}H and ^{13}C) or external tetramethylsilane (^{29}Si).

In a 500 mL jacketed reactor, $(isobutyl)_7Si_8O_{12}$(propyl methacrylate) (40.0 g, 0.0424 mol), methyl methacrylate (120.0 g, 1.199 mol), 0.25 mole % AIBN (0.509 g, 3.10 mmol) and toluene (124 mL) were loaded under a nitrogen atmosphere to produce the isobutyl-POSS copolymer $CP_{iBu25Hi}$. The jacketed part of the reactor was filled with heating fluid maintained at 60 °C and the reaction mixture stirred under a nitrogen atmosphere. Overnight the solution became very viscous. After 40 hours, the reactor was opened to air, diluted with $CHCl_3$ (200 mL) and allowed to stir overnight to form a less viscous solution. This was slowly poured through a small bore funnel into well-stirred methanol. A fibrous polymer was formed around the stir bar. After the addition was complete, the polymer was stirred for another hour before it was removed from the methanol/toluene mixture and dried overnight at 40 °C under vacuum. A nearly quantitative yield of 158.1 grams of copolymer was isolated. A ^{1}H NMR spectrum was obtained to show that no residual unreacted POSS monomer was present (demonstrated by the absence of any peaks in the 5-6.5 ppm olefin region of the spectrum). Integration of the ^{1}H NMR spectra indicated that the mole % POSS in the copolymer (3.4 mole %) was the same as the % POSS in the monomer feed. The same synthesis procedure was used to produce the cyclopentyl version of the copolymer (CP_{Cp25}) and the high molecular weight homopolymer (HP_2). The amounts of reagents used to synthesize CP_{Cp25} were: $(cyclopentyl)_7Si_8O_{12}$(propyl methacrylate) (40.0 g, 0.0389 mol), methyl methacrylate (120.0 g, 1.199 mol), 0.25 mole % AIBN (0.508 g, 3.09 mmol) and toluene (124 mL). A yield of 156.1 grams of copolymer was isolated. ^{1}H NMR spectra confirmed that the copolymer was monomer-free and that the mole % POSS in the copolymer (3.1 mole %) was the same as the % POSS in the monomer feed. The amounts of

reagents used to synthesize the homopolymer HP_2 were: methyl methacrylate (125.0 g, 1.249 mol), 0.25 mole % AIBN (0.513 g, 3.12 mmol) and toluene (125 mL). A yield of 123.4 grams of copolymer was isolated. ^{1}H NMR spectra confirmed that the homopolymer was monomer-free. Molecular weight (M_w) and polydispersity (PDI) values for the copolymers and the homopolymer (Table 1) were determined using a Waters Gel Permeation Chromatograph (GPC) on a polystyrene standard with THF as eluent.

A commercial PMMA resin from Atofina Chemicals (Atoglas V920, HP) was used for homopolymer blends due to its stability at high temperatures. A copolymerized PMMA containing 15 wt% tethered isobutyl-POSS (CP_{iBu15}) was purchased from Hybrid Plastics and a PMMA copolymer containing 25wt% tethered isobutyl-POSS (CP_{iBu25}) was purchased from Sigma-Aldrich for use in blend characterization. Molecular weight and polydispersity values for these polymers are reported in Table 1.

Two different POSS fillers [isobutyl-POSS (F_{iBu}) and cyclohexyl-POSS (F_{Cy})] were purchased from Hybrid Plastics. The molecular weights of these fillers are 873.6 and 1081.9 g/mol, respectively. The crystalline density of cyclohexyl-POSS was reported to be 1.174 g/cm^3 by Barry et al.[20] The value for isobutyl-POSS has not been reported, but Larsson reported crystal densities for many POSS cages with similar structure.[21] For (n-propyl)-POSS, two crystal forms are present and the densities for these are 1.09 and 1.20 g/cm^3. For isopropyl-POSS, a density of 1.20 g/cm^3 was given, and for (n-butyl)-POSS a crystal density of 1.14 g/cm^3 was reported. These data suggest that isobutyl-POSS should have a density at least as high as that of (n-butyl)-POSS. However, as will be shown in the Results section, isobutyl-POSS has two crystal structures, which, if similar to (n-propyl)-POSS, would have different but similar densities. An estimate of 1.15 g/cm^3 was thus taken as a reasonable median value for the isobutyl-POSS filler's density. This value and the crystal density of the cyclohexyl-POSS are very close to the density of the PMMA homopolymer, ρ_{PMMA} = 1.17 g/cm^3.

Blend Preparation

Each of the filler species (cyclohexyl-POSS and isobutyl-POSS) were blended separately with PMMA in a DACA Instruments micro-compounder at 220°C for five minutes at compositions between 1 and 30 vol%. The isobutyl-POSS filler (F_{iBu}) was also blended with the

low molecular weight isobutyl-POSS copolymer (CP_{iBu25}) at 175°C for five minutes at compositions between 2 and 35 vol%; the lower temperature was required to minimize thermal degradation of the copolymer. Rheological samples were made by compression-molding the extruded samples into disks 25 mm in diameter with a thickness of 2 mm. Molding temperatures were 190°C for the homopolymer blends and 150°C for the copolymer blends.

X-ray Scattering

Wide angle x-ray diffraction (WAXD) was carried out on two different diffractometers. Room temperature tests were performed on a Rigaku RU300 18kW rotating anode generator with a 250 mm diffractometer. Tests at low and high temperature were performed in a Siemens 2D Small Angle Diffractometer configured in Wide Angle mode using a 12kW rotating anode; these samples (powders mounted on Kapton tape) were tested in transmission. CuK_{α} radiation was used in both cases.

Differential Scanning Calorimetry (DSC)

Thermal analysis was performed on a TA Instruments Q1000 DSC. Samples were heated at 5°C/min, cooled at the same rate, and then data was collected on the second heating ramp at the same heating rate. Glass transition temperatures (T_g) were determined from the inflection point in the heat flow vs. temperature curves. Melting points (T_m) and latent heats (ΔH) of the isobutyl-POSS-filled homopolymer blends (F_{iBu}/HP) were determined from the peak and the area of each melting endotherm, respectively.

Rheological Characterization

Rheological tests were performed on two separate rheometers. Linear viscoelastic tests of the high molecular weight homopolymer (HP_2) and the high molecular weight copolymers (CP_{iBu15}, $CP_{iBu25Hi}$ and CP_{Cp25}) were performed on a Rheometrics RMS-800 strain-controlled rheometer at strains between 0.1 and 1%, and at temperatures between 140°C and 220°C. All blend samples were rheologically characterized using a TA Instruments AR2000 stress-controlled rheometer. The filler-homopolymer blends were tested between 140°C and 225°C; the filler-copolymer blends were tested between 120°C and 170°C. All rheology samples were tested in air using 25 mm parallel plates with gap sizes of approximately 2 mm.

Results

Characterization

X-ray diffraction patterns taken at room temperature for the cyclohexyl-POSS-filled homopolymer (F_{Cy}/HP) and the isobutyl-POSS-filled copolymer (F_{iBu}/CP_{iBu25}) blend systems are shown in Figure 2. From Figure 2(a) it is clear that even at the lowest loading of 1 vol% filler ($1F_{Cy}$/99HP) appreciable POSS crystallinity is present in the homopolymer blends. There is strong correspondence between the peak patterns of the blends and that of the pure POSS powder, and the peak locations agree with the results of Barry et al.[20] for cyclohexyl-POSS within 0.01 nm. Sharp crystalline peaks were also observed at room temperature in the isobutyl-POSS-filled homopolymer blend system (F_{iBu}/HP) for all blend compositions.

The WAXD pattern for the copolymer CP_{iBu25} in Figure 2(b) shows no sharp peaks, only a slight hump at $d = 0.97$ nm. This result is consistent with previous WAXD studies of polymers containing tethered-POSS at comparable weight fractions.[10,13] At 5 vol% isobutyl-POSS, a broad peak forms which spans the 2θ range of the two highest peaks in the POSS powder spectrum ($7.5° < 2\theta < 9°$). At higher loadings, the peak pattern closely resembles that of the POSS powder; however, the peak height ratios differ between the POSS powder and the blends. In the isobutyl-POSS powder, the first peak ($d = 1.12$ nm) is double the height of the second peak ($d = 1.01$nm); but in the 35 vol%-filled copolymer, the first peak is only about 15% higher. This suggests that there are two crystal forms present in the isobutyl-POSS filler, with the ratios of the crystal structures differing between the blends and the POSS powder. Larsson[21] reported two crystal

forms for (n-propyl)-POSS, stating that the two forms differ in the packing of the propyl groups in the crystal.

Comparison of the 5 vol%-cyclohexyl-POSS-filled homopolymer ($5F_{Cy}$/95HP) WAXD pattern and that for the 5%-isobutyl-POSS-filled copolymer ($5F_{iBu}/95CP_{iBu25}$) shows that, at low filler loadings, there are substantially larger POSS crystals in the homopolymer blend. While the relative extents of crystallinity between the two types of blends are not easily determined from WAXD, the absence of any sharp peaks in the $5F_{iBu}/95CP_{iBu25}$ blend suggests better nanodispersion of untethered-POSS at low loadings in the filled copolymer blend system compared to the filled homopolymer systems.

X-ray diffraction was also performed at elevated temperatures using a separate diffractometer to investigate the stability of the two crystalline phases of isobutyl-POSS. Figure 3 shows diffraction patterns for the isobutyl-POSS filler ($100F_{iBu}$) at temperatures of 30°C and 110°C. It is clear that one of the diffraction peaks (near $2\theta = 9°$) disappears at the higher temperature, and the high-angle peak ($2\theta = 20°$) is greatly diminished in sharpness and height. From Fig. 2(b) it is evident that the lower melting crystal corresponds to the $d = 1.01$ nm peak, while the higher melting crystal corresponds to the $d = 1.12$ nm peak. Therefore, based on the relative peak heights seen in Figure 2(b), in the blends there is an enrichment of the lower melting crystal compared to that found in the pure isobutyl-POSS filler. This portion of the isobutyl-POSS is amorphous in the rheological temperature range used for the F_{iBu}/HP blends ($140°C < T < 225°C$) and the F_{iBu}/CP_{iBu25} blends ($120°C < T < 170°C$).

The melting behavior of the blends was quantified using DSC, and representative curves for the isobutyl-POSS-filled homopolymer blend system (F_{iBu}/HP) are reproduced in Figure 4. In the pure isobutyl-POSS filler ($100F_{iBu}$), there are two melting transitions: a sharp one at 60°C and a broader one at 261°C. Similar results are seen in the F_{iBu}/HP blends, with the lower melting point shifted to lower temperatures and the higher melting point shifted to higher temperatures compared to the pure isobutyl-POSS filler. The endotherms increase in magnitude with increasing POSS content and the peaks become sharper. Melting points(T_m) and latent heats normalized by POSS content ($\Delta H/g_{POSS}$) are reported in Table 2. In Figure 5 we show the heat of fusion per gram of isobutyl-POSS filler in the samples as a function of POSS content. The horizontal dashed lines correspond to ΔH_1^* and ΔH_2^*, which are the specific heats of fusion for the isobutyl-POSS filler. If the isobutyl-POSS had the same degree of crystallinity in the

homopolymer blends as in its pure form the data would not change with increasing POSS content. However, the data show an increase in the heat of fusion per gram of POSS filler ($\Delta H/g_{POSS}$) with increasing POSS content. The region of steepest increase is below 10 vol%. This suggests that at low loadings a large fraction of the POSS enters the polymer matrix as amorphous particles. As the concentration of filler increases, a limiting value corresponding to the pure POSS powder is approached from below. This implies a solubility limit of POSS nanoparticles exists in the PMMA matrix. Similar results were found for the isobutyl-POSS-filled copolymer blend system (F_{iBu}/CP_{iBu25}), however the second melting point of the filler ($T \sim$ 260°C) could be not be reached before extensive thermal degradation occurred. The cyclohexyl-POSS powder (F_{Cy}) showed no melting transition below 400^0C and thus no melting of filler was observed in the F_{Cy}/HP system.

Values of the glass transition temperature (T_g) were also obtained from the DSC curves. Table 4 shows that in both filled homopolymer blend systems (F_{Cy}/HP and F_{iBu}/HP) there was no significant change in the glass transition temperature of the blends over the range of filler loadings. In the filled copolymer system (F_{iBu}/CP_{iBu25}), whose T_g values are reported in Table 5, there was no change for volume fractions $\phi \leq 20\%$ before an 8°C jump was seen in the 30 vol%-filled blend.

Rheology

In Figure 6 we show master curves for the storage modulus G' and the loss modulus G'' at $T_0 = 170$°C for four unfilled polymers: a high molecular-weight homopolymer (HP_2), and three highly entangled copolymers (CP_{iBu15}, $CP_{iBu25Hi}$, and CP_{Cp25}). The storage moduli show a significant shift downward and to the right with the addition of POSS to the chain. The magnitude of the storage modulus is similar for all three copolymers even though they exhibit significantly different glass transition temperatures (Table 3) that bracket the homopolymer's T_g. Approximate plateau moduli (G_N^0) were calculated using the convention:[22,23]

$$G_N^{\,0} = \left(G'(\omega)\right)_{\tan\delta \to \min} \qquad (2)$$

where the plateau modulus is taken as the point in the storage modulus where the loss tangent $\tan\delta = G''/G'$ is at a minimum. Values of entanglement molecular weight, M_e, were then calculated from the expression:[24]

$$M_e = \left(\frac{4}{5}\right)\frac{\rho RT}{G_N^{\,0}} \qquad (3)$$

These values are tabulated in Table 3 along with $Z = M_w/M_e$, the number of entanglements per chain. The plateau modulus for PMMA ($G_N^0 = 5.2 \times 10^5$ Pa) at $T_0 = 170$°C agrees with the values reported in Fuchs et al., which ranged from $4.6 \times 10^5 \le G_N^0 \le 6.1 \times 10^5$ Pa at $T_0 = 190^0$C.[25] The data reported by Fuchs et al. were for monodisperse PMMAs with the exception of the lowest plateau modulus value, which was for a PMMA with a polydispersity PDI = 2.0, similar to that for HP_2 in this study. The terminal region and zero-shear-rate value of the viscosity for these PMMA copolymers could not be readily accessed due to thermal instability at high temperatures: HP_2, CP_{iBu15} and $CP_{iBu25Hi}$ all depolymerized at temperatures above 200°C, leading to foaming of the samples; CP_{Cp25} crosslinked above 200°C, causing a low frequency plateau in the storage modulus G' and rendering the sample insoluble in THF.

The poor thermal stability of these polymers for extended times at high temperature led to the use of different matrix materials for the blend portion of the study. In particular, a copolymer (CP_{iBu25}) with substantially lower molecular weight (see Table 1) was used to study the effect of blending isobutyl-POSS filler with copolymer. In Figure 7 we show linear viscoelastic moduli for blends of isobutyl-POSS and copolymer (F_{iBu}/CP_{iBu25}) at a reference temperature $T_0 = 150$°C for filler loadings between 0 and 30 vol%. The storage and loss moduli G' and G'' increase monotonically but retain the same shape up to a filler loading of 20 vol%, with a noticeable change in the terminal slope for the 30 vol%-filled sample. This change in the blend's relaxation spectrum is consistent with the discontinuity in the T_g values obtained from DSC (Table 5). There is also evidence of failure of time-temperature superposition (TTS) at low frequencies for the 30 vol%-filled sample. Zero shear viscosities were calculated from the relation:

$$\eta_0 = \lim_{\omega \to 0}\left(\frac{G''}{\omega}\right) \qquad (4)$$

and are reported in Table 5.

In Figure 8 we show the linear viscoelastic moduli for the homopolymer (HP) and two blends of homopolymer with 5 vol% POSS filler ($5F_{iBu}$/95HP and $5F_{Cy}$/95HP) at $T_0 = 190$°C. In contrast to the response observed with the filled copolymer, there is virtually no change in the storage modulus G' or the loss modulus G'' of the 5 vol% cyclohexyl-POSS-filled homopolymer. The curves for the isobutyl-POSS-filled homopolymer contain a less-sustained plateau region

than what is observed in either the pure homopolymer or the cyclohexyl-POSS-filled sample and thus the values of G' and G'' are noticeably lower for the isobutyl-POSS-filled homopolymer in the terminal region. This melt softening is caused at least in part by that filler's first melting transition at $T = 60°C$. As we discuss further below, the lack of reinforcement of the linear viscoelastic moduli at low loadings is indicative of a true nanodispersion of the POSS in the PMMA matrix at low volume fractions of filler. This behavior can be contrasted with that shown in Fig. 9 for higher volume fractions of cyclohexyl-POSS ($\phi \geq 10\%$). A substantial increase in G' is seen at these higher loadings, more indicative of conventional rigid filler behavior. The 30 vol% cyclohexyl-POSS-filled data appear to enter a plateau region at frequencies $a_T\omega < 10^{-3}$ rad/s at $T_0 = 190°C$. The isobutyl-POSS-filled homopolymer system exhibits qualitatively similar behavior at high filler loadings with a less substantial enhancement in G'. Fu et al. observed similar solid-like behavior at low frequencies in an ethylene-propylene copolymer filled with comparable amounts of methyl-POSS (~30 wt%).[15] These results contrast somewhat with the results of Romo-Uribe et al. for tethered-POSS copolymers, which showed no solid-like behavior at low frequencies for loadings less than 45 wt% tethered-POSS.[10] The relationship between volume fraction and weight fraction is not clear in tethered-POSS-containing copolymers, but the differences are likely not large. Thus it appears that untethered-POSS induces percolation in polymer melts at lower volume fractions than tethered-POSS.

Discussion

We now seek to understand the systematic trends observed in the thermal and rheological data with respect to the triangular composition diagram in Figure 1. Firstly, in the inset of Figure 6(a) we show a qualitative trend of increasing entanglement molecular weight M_e with increasing POSS content based on plateau modulus values for the isobutyl-POSS copolymers CP_{iBu15} and $CP_{iBu25Hi}$. This trend is consistent with the results of Romo-Uribe et al.,[10] who showed that tethered-POSS substantially decreases the zero-shear-rate viscosity of weakly entangled polymers at a given molecular weight. This suggests that tethered-POSS, due to its compact size (d~1.5 nm) and relatively small molecular weight (M~1000 g/mol), reduces the entanglement density in a way analogous to short-chain branches in branched polymers.[26] In addition to reducing the linear viscoelastic moduli, tethered-POSS also shifts the curves to higher frequencies (shorter times), thereby accelerating chain relaxation processes.

In Figure 10 we plot approximate plateau modulus values $G_N^0(\phi)$ [normalized by the homopolymer's plateau modulus $G_N^0(0)$], calculated using Equation 2, for all three blend systems. For the two filled homopolymer systems an essentially constant plateau modulus persists at low volume fractions of filler ($\phi \leq 5$ vol%) before an upturn appears at higher loadings. The plateau modulus values at higher loadings are greater for cyclohexyl-POSS-filled homopolymer than in the equivalent isobutyl-POSS-filled homopolymer blends, likely due to the isobutyl-POSS filler's low temperature melting transition ($T \sim 60°C$). Data were compared to predictions for hard sphere fillers from the Guth-Smallwood Equation:[27]

$$G_N^0(\phi_e) = G_N^0(0)\left(1 + 2.5\phi_e + 14.1\phi_e^2\right) \quad (5)$$

where ϕ_e is the effective volume fraction of particles. A superb fit was obtained for the cyclohexyl-POSS-filled homopolymer system by setting the effective volume fraction $\phi_e = \phi - 3$. Thus the first 3 vol% of filler has no apparent effect on G_N^0 and above 3 vol% the filler behaves as a hard sphere. Like the DSC data in Fig. 5, this implies a region of significant nanodispersion at low loadings until a solubility limit is reached, at which point virtually all added POSS filler agglomerates into crystallites. From Fig. 3(a) it is clear that there is some cyclohexyl-POSS crystallinity even at a loading of 1 vol%, but the nanodispersed portion of the filler at loadings $\phi \leq 5$ vol% softens the melt to offset the reinforcement expected by the crystallites. The filled copolymer system (F_{iBu}/CP_{iBu25}) exhibits similar behavior, showing a monotonic increase in G_N^0 for all loadings, and in particular an increase at low loadings that fits Equation 5 quite well for $\phi_e = \phi$. Thus the copolymer experiences a hard-sphere-like reinforcement when filled with untethered-POSS particles, suggesting that the POSS domains have aspect ratios close to 1.

A variety of studies have examined the effect of filler on a homopolymer's plateau modulus. Poslinski et al.[28] blended 15 μm glass spheres with a high molecular-weight thermoplastic polymer and found an increase in the plateau modulus similar to what is seen in the F_{Cy}/HP system (see Fig. 10). Friedrich et al.[29] filled polystyrene melts with 10 μm glass spheres and observed a less-substantial increase in the plateau modulus with increasing particle content; the relative plateau modulus $G_N^0(\phi)/G_N^0(0)$ increased to approximately 1.8 at a particle volume fraction of $\phi = 30\%$. No data for suspensions in the range $0 < \phi < 10\%$ were reported in either study. Yurekli et al.[30] examined a modified polyisobutylene filled with carbon-black and reported a relative plateau modulus $G_N^0(\phi)/G_N^0(0) \sim 6.0$ at 20 vol% carbon black loading, much

larger than what is predicted by Eq. 5. However, when a modified form of Eq. 5 was used which incorporated the filler aspect ratio, the data of Yurekli et al. were more closely followed.

In Figure 11 we plot the normalized zero-shear-rate viscosities [$\eta_0(\phi)/\eta_0(\phi)$] for the blends in an analogous fashion to the plateau moduli in Figure 10. The filled homopolymer systems show an initial decrease in the zero-shear-rate viscosity at loadings less than 5 vol%. This result is significantly different from the prediction of the Einstein-Batchelor equation for hard sphere suspensions (shown by the dotted line in Fig. 12):[31]

$$\eta_0(\phi_e) = \eta_0(0)\left(1 + 2.5\phi_e + 6.2{\phi_e}^2\right) \qquad (6)$$

which predicts a monotonic increase in viscosity with increasing particle loading. A decrease in viscosity with particle loading has been shown in polystyrene melts filled with 5 nm crosslinked polystyrene particles by Mackay et al.;[17] however, that study showed no clear trend in viscosity with increasing particle loading. The present data show a well-defined upwards curvature to the viscosity-filler loading curve for the filled homopolymer, consistent with an initial regime of nanoparticle plasticization followed by reinforcement by rigid crystallites. For comparison, data from Poslinski et al.[28] for a glass bead-filled thermoplastic are plotted in Fig. 11. The lowest loading investigated ($\phi \sim 12\%$) is close to the prediction of Eq. 6, but the points at higher loading diverge upward from the curve. The data for the filled homopolymer blends (F_{Cy}/HP and F_{iBu}/HP) appear to approach the same diverging behavior, however zero-shear-rate viscosities for loadings above 10 vol% could not be obtained due to the appearance of yield stress effects.

The decrease in viscosity at low loadings in the homopolymer blends and the eventual increase at higher loadings is again consistent with the combined presence of nanodispersed filler and crystallites. Figure 13(a) illustrates this concept. Initially an appreciable fraction of the POSS particles enter the matrix as amorphous, molecularly dispersed particles, and another fraction goes in as crystalline aggregates. The molecularly-dispersed particles act as a plasticizer, increasing the free volume due to the local mobility of the pendant R-groups and thereby decreasing the viscosity of the blend, but at higher loadings ($\phi \geq 5\%$) a saturation limit is reached regardless of compounding history. At this point any additional POSS filler agglomerates into crystallites, which increase the viscosity in a way analogous to hard spheres. The DSC data in Figure 5 show that the fraction of isobutyl-POSS present as amorphous material is higher at the lower loadings (ϕ<10%) than at higher loadings. In the F_{Cy}/HP system, for which there is no melting transition within the rheological or processing temperature range (140°C ≤ T ≤ 225°C),

more of the filler is incorporated into crystallites than in the F_{iBu}/HP system [see Fig. 3(a)] and the decrease in viscosity as a result of plasticization is less substantial.

By contrast, the filled copolymer blend system (F_{iBu}/CP_{iBu25}) shows a substantial increase in the zero-shear-rate viscosity for all loadings (Figure 11). This enhancement is significantly greater than that predicted by Equation 6. However, a superb fit is obtained if the effective volume fraction occupied by a POSS filler cage in the melt is allowed to the exceed the actual volume fraction by a factor $\phi_e = 2.75\phi$ (indicated by the dashed line in Fig. 11). This result is not surprising when one considers that in the blend of 5% isobutyl-POSS with the copolymer ($5F_{iBu}CP_{iBu25}$), the mole ratio of untethered POSS groups to tethered-POSS groups in the blend ($N_{Untethered}/N_{Tethered\ POSS}$) is only 0.23 (see Table 5), meaning the untethered-POSS filler constitutes only 23% of the total POSS contained in the blend. Therefore, especially at low filler loadings, the untethered-POSS is expected to strongly associate with the tethered-POSS and thereby increase the effective volume fraction of the filler, leading to the factor of 2.75 multiplied by the volume fraction in fitting the data to Equation 6.

The trends observed in the plateau moduli and the zero-shear-rate viscosities are qualitatively similar. The enhancement in each material property is greater in the filled copolymer compared to the two filled-homopolymer systems, illustrating a stronger matrix-filler interaction facilitated by the tethered-POSS attached to the matrix. To more clearly show the differences between the two types of blend systems, both horizontal and vertical concentration shift factors (a_ϕ and b_ϕ, respectively) were computed by shifting the storage modulus curves for the blend samples onto the respective unfilled polymer's master curve. The quality of the shifts for the filled copolymer system is shown in the inset to Fig. 7(a). In Figure 12 we plot both the horizontal shift factors a_ϕ (open symbols) and vertical shift factors b_ϕ (closed symbols) for both the filled homopolymer and the filled copolymer blend systems. No vertical shifts are required in the filled homopolymer blends for $\phi \leq 5\%$, however the filled copolymer blend requires vertical shifts at all filler loadings in order to superpose onto the unfilled copolymer's master curve. All blends above $\phi = 10\%$ require significant vertical shifts and thus the trend of increasing vertical shifts with filler loading is similar in the filled homopolymer blends and the filled copolymer blends. The horizontal shift factors a_ϕ, however, display a stark contrast between the blend systems. Only minimal horizontal shifting is required in the filled homopolymer blend systems, whereas in the filled copolymer a linear increase in a_ϕ with a slope of 7.5 is observed with

increasing filler content. Thus for every 13 vol% of untethered-POSS added to the copolymer a subsequent one decade increase in relaxation time is observed.

It is insightful at this point to utilize the Doi-Edwards scaling relation for the viscosity of entangled polymers:

$$\eta_0 \cong G_N^{\,0} \tau_{rep} \qquad (7)$$

where τ_{rep} is the reptation time of the polymer. To a first approximation, filler particles may be expected to reinforce a polymer melt, which would increase the plateau modulus G_N^0, or to retard chain motions, which would increase τ_{rep}. Overall, the reinforcement is more substantial in the filled copolymer systems (see Fig. 10), but both the filled homopolymer and the filled copolymer systems show a significant reinforcement effect which closely follow the prediction of Eq. 5. The retardation term, which is directly related to the horizontal shift factor a_ϕ, is not significantly affected in the untethered-POSS-homopolymer blend systems, but it linearly increases with filler loading in the copolymer blends. The rheological data in Figure 6 for unfilled copolymers show clearly that tethered-POSS, in the absence of untethered-POSS filler, does not retard chain relaxation, and in fact speeds it up. Thus the additional retardation term gleaned from a_ϕ must be due to associations between tethered-POSS and untethered-POSS particles in the blend, which significantly slow the chain relaxation processes. This is largely responsible for the large increase in the zero-shear-rate viscosity shown in Figure 11. An unusual aspect of this result is that the storage and loss moduli G' and G'' show virtually no change in shape up to 20 vol% filler loading. In other filled systems with attractive matrix-filler interactions such as carbon-black-filled elastomers,[30] silica-filled poly(ethylene oxide),[16] and clay-filled polystyrene-*g*-maleic anhydride,[33] a sustained plateau in $G' \geq 10^4$ Pa typically persists at low frequencies for loadings $\phi \geq 10\%$. This solid-like behavior is indicative of a particle network which has percolated throughout the structure of the sample. There is ample evidence which suggests that percolation does not occur in the F_{iBu}/CP_{iBu25} system until 30 vol% isobutyl-POSS filler is added (shape of the linear viscoelastic moduli and glass transition temperatures); however, the linear increase in horizontal shift factor a_ϕ is present at all loadings. Thus the retardation caused by the thermodynamic interaction between the tethered and untethered isobutyl-POSS appears to be a local effect restricted to isolated nanoscopic domains within the sample (see Fig. 13(b)). This is plausible when it is noted that the mole fraction of tethered-POSS in the copolymer CP_{iBu25} is only 3.4%. Thus only one out of every 29.4 repeat units in the copolymer contains a covalently

tethered isobutyl-POSS particle. The relatively long PMMA connectors have no specific attraction to the isobutyl-POSS, as evidenced by the plasticization at low loadings, and thus they are not strongly perturbed by the POSS domains. This substantially lessens the effect of chain adsorption, which is a primary cause of percolation in nanocomposite systems with attractive matrix-filler interactions.[16] Therefore at low to moderate loadings of untethered-POSS in the copolymer, a network of largely-unperturbed PMMA domains exists, allowing bulk relaxation in the presence of the nanoscopic POSS domains. At filler loadings $\phi \geq 20\%$, the untethered-POSS becomes the dominant POSS species in the system and thus the tethered-POSS groups become saturated in their nanoscopic associations with untethered-POSS. This leads to the formation of large amounts of crystallites, which perturb the PMMA matrix and lead to percolation throughout the sample.

Time-Temperature Superposition

The addition of unbound POSS nanofiller into an entangled polymer matrix may result in several competing effects. The high local mobility of the pendant R-groups on the Si_8O_{12} cages will create free volume and thus locally plasticize the matrix, leading to enhanced molecular mobility; conversely, the addition of a rigid filler (albeit nanoscale in characteristic dimension) is expected to result in enhanced local dissipation with a less clear effect on free volume. In the case of the covalently-bound POSS in the copolymer system, the expected effect of additional filler is even more complex. The effects of local plasticization will already have been incorporated by the original copolymerized POSS moieties (see Figure 6). Associations between tethered-POSS groups also incorporate untethered-POSS filler. The expected effect of the filler on the copolymer's free volume is not obvious, since the copolymer's tethered-POSS would presumably already affect the free volume analogously to what is expected from the untethered-POSS, but the effect would presumably be similar to that expected for the homopolymer, in which the compact POSS molecules increase the free volume.

The TTS shift factors were analyzed to further investigate the contrasting trends in the zero-shear-rate viscosities η_0 of the homopolymer and copolymer blends. Time temperature shift factors $a_T(T, T_0)$ were obtained by shifting $tan\ \delta$ curves obtained over a range of temperatures to a reference temperature (T_0 = 190°C for the homopolymer, T_0 = 135°C for the copolymer). To illustrate the quality of the TTS an example is given in Figure 14. In Figure 14(a) we plot the

unshifted *tan* δ curves for the 10 vol% cyclohexyl-POSS-homopolymer blend and in Figure 14(b) we show the curves after shifting. No subsequent vertical shifting was required.

The shift factors were initially plotted against 1/T to determine whether the samples followed Arrhenius behavior; however, high correlation coefficients were only obtained at high temperatures ($T \geq 190$°C), so the WLF equation was employed in order to capture the thermal dependence of the shift factor data over the entire temperature range:[34]

$$\log a_T = \frac{-c_1^0 (T - T_0)}{c_2^0 + (T - T_0)} \qquad (8)$$

WLF coefficients were calculated by plotting the quantity $-(T\text{-}T_0)/\log a_T$ against $(T\text{-}T_0)$ at $T = T_0$;[34] c_1^0 was obtained from the reciprocal of the slope, and c_2^0 from the intercept. An example of the use of this method can be found in the work of Fetters et al. for polyisobutylene melts.[35] Values of the WLF coefficients are reported in Table 4 for all filler-homopolymer blends. The value of $c_1^0 = 8.6$ obtained for the PMMA homopolymer agrees with values reported by Fuchs et al for PMMA homopolymers ($8.6 \leq c_1^0 \leq 9.4$).[25]

A representative WLF plot for the cyclohexyl-POSS-homopolymer blend system is given in Figure 15(a), one set of data corresponding to the unfilled homopolymer and another for a blend containing 10 vol% cyclohexyl-POSS. There is a small but reproducible difference in the slope and the location of the two lines, indicating changes in the respective WLF coefficients. The c_1^0 values can be related to the fractional free volume f_0 using the relation:[34]

$$f_0 = \frac{B}{2.303 c_1^0} \qquad (9)$$

where B is a constant usually assumed to be unity. Values of f_0/B are reported in Table 4 along with the zero-shear-rate viscosities for the homopolymer blends. Surprisingly, for filler loadings $\phi \leq 5\%$, the fractional free volume of unfilled homopolymer obtained from TTS (0.050) is larger than that of the cyclohexyl-POSS-homopolymer system (0.048) but smaller than that of the isobutyl-POSS-homopolymer system (0.051-0.052). The difficulty in developing clear trends lies in the above-mentioned competition between molecular dispersion and crystalline aggregation, which is present at all loadings (see Figure 2(a)). The decrease in viscosity seen at low loadings in the filler-homopolymer system is almost certainly a result of additional free volume generated by the dispersed POSS nanoparticles, whose mobile, pendant R-groups are expected to create appreciable void space; the WLF coefficients in the F_{Cy}/HP system do not support this trend because of the complication caused by the crystallites, which reinforce the melt and thereby

skew the WLF coefficients to values which suggest an opposing trend. The effect of the crystallites can be demonstrated by analyzing the coefficients obtained in the F_{Cy}/HP system. Up to 10 vol% cyclohexyl-POSS filler, the first WLF coefficient shows a monotonic increase from $c_1^0 = 8.6$ for the homopolymer to $c_1^0 = 9.9$ for the 10%-filled sample. But the 20%-filled sample has a c_1^0 value of only 7.6, substantially smaller than the homopolymer's value, which leads to a higher calculated fractional free volume value (0.057). Nothing in the linear viscoelastic data in Fig. 9 or in the T_g values in Table 5 predict such a change in molecular arrangement. Future rheological studies on a POSS-filled system in which crystallization is entirely absent or at least greatly suppressed would help to clarify the interesting role of molecularly-dispersed POSS on the thermorheological properties.

In Figure 15(b) we show the WLF plot for the unfilled copolymer and the copolymer filled with 5 vol% isobutyl-POSS filler. Untethered-POSS clearly has a stronger effect at low loadings ($\phi \leq 5\%$) on the time-temperature behavior in the copolymer blends. The slope of the $5F_{iBu}/95CP_{iBu25}$ line is notably larger, leading to smaller c_1^0 and c_2^0 values. The WLF coefficients for the filled copolymer system are reported in Table 5. In the range of isobutyl-POSS loadings $2\% \leq \phi \leq 20\%$, increasing the amount of POSS filler increases both the fractional free volume f_0 and the zero-shear-rate viscosity η_0. In particular, at loadings of $\phi \leq 5\%$, which contain only small amounts of crystallite content [see Figure 2(b)], the fractional free volume increases from $f_0/B = 0.048$ for the unfilled copolymer at $T_0 = 135°C$ to $f_0/B = 0.065$ for the copolymer blended with 5 vol% isobutyl-POSS. That the free volume and viscosity should both increase is counter to the concepts introduced by Doolittle which relate free volume in liquids to viscosity.[36] However, our result is not unreasonable, as the thermodynamic attraction between the well-dispersed isobutyl-POSS filler and the tethered-isobutyl-POSS groups in the copolymer chain could offset the increase in free volume observed in the system. The significant nanodispersion of the untethered-POSS in the copolymer system, evidenced both by the X-ray pattern for the $5F_{iBu}/95CP_{iBu25}$ blend in Figure 2(b) and the strong retardation of chain motion evident from the linear viscoelastic data, is responsible for the observed increase in free volume.

Tables 4 and 5 also report values of f_g/B, the fractional free volume at the glass transition temperature. These were calculated using a relation adapted from Ferry:[30]

$$f_g = \frac{B\left(c_2^0 + T_g - T_0\right)}{2.303 c_1^0 c_2^0} \qquad (10)$$

where c_1^0 and c_2^0 are the WLF coefficients determined at T_0. While no new trends or insights are obtained from this transformation, the numerical values of f_g provide support for the validity of the time-temperature superposition scheme, particularly for the POSS-filled homopolymer systems. According to Ferry, WLF coefficients, when referenced to the glass transition temperature, should lead to a numerical value of f_g in the range 0.025 +/- 0.005 for all systems, and all but one of the highly loaded compounds in Table 4 conforms to this paradigm. The values of f_g for the compounds based on CP_{iBu25} lie somewhat above the universal range.

Conclusion

Poly(methyl methacrylates) containing both tethered and untethered polyhedral oligomeric silsesquioxanes (POSS) were investigated using wide-angle X-ray diffraction, differential scanning calorimetry, and rheological characterization. Entangled linear copolymers containing tethered-POSS showed a decrease in the plateau modulus compared to the homopolymer and this trend was nearly the same for two 25wt% POSS copolymers with different R-groups. This behavior was attributed to the tethered-POSS behaving analogously to a short-chain branch, thereby reducing the entanglement density and softening the polymer in the melt state.

Wide angle x-ray diffraction (WAXD) showed significant crystallinity of untethered-POSS when it was blended with PMMA homopolymer even at loadings as low as 1 vol%, while significant crystallinity in the filled copolymer blends was not observed until greater than 5 vol% filler had been added. Melting endotherms from DSC suggest a regime at low loadings (≤ 5 vol%) in which a large fraction of untethered-POSS enters the homopolymer in an amorphous state before a solubility limit is reached, at which point virtually all additional POSS filler is incorporated into crystallites.

Contrasting behavior was observed between the rheology of untethered-POSS-homopolymer blends and the untethered-POSS-copolymer blends. A minimum in the zero-shear-rate viscosity and a constant plateau modulus at loadings below 5 vol% were seen for both the isobutyl-POSS-filled and the cyclohexyl-POSS-filled homopolymer, indicating an initial plasticization of the matrix by the untethered POSS filler. However, at higher loadings these values increased in a way consistent with hard sphere fillers. Combining the thermal and rheological data leads to the conclusion that untethered-POSS distributes in two ways in a

homopolymer matrix: as molecularly dispersed nanoparticles and as crystallites. The copolymer blends showed a substantial increase in viscosity at all loadings. This was attributed to a substantial retardation of chain relaxation processes caused by significant association between the POSS cages on the chains and those in the blend. This thermodynamic attraction is particularly effective at retarding chain motions in nanoscopic domains while still allowing macroscopic relaxation of the sample.

Time-temperature superposition (TTS) was used to determine whether the decrease in viscosity in the untethered-POSS-homopolymer blends could be correlated with an increase in free volume. Linear regression fits to the WLF equation were excellent, however there was no strong trend in the coefficients for the homopolymer blends. This was due to the POSS filler's tendency to form crystallites, which became dominant at filler loadings above 5 vol%. The untethered-POSS-copolymer blend system shows a significant decrease in the WLF coefficients upon the addition of small amounts of untethered-POSS filler, suggesting an increase in free volume with filler loading. Surprisingly, the viscosity also increases dramatically in this region; however, this counterintuitive result can be explained by the strong thermodynamic interaction between tethered and untethered-POSS moieties, which more than offsets the plasticization caused by the free volume increase.

Acknowledgements

This research was sponsored by the DURINT project of the U.S. Air Force under grant number F49620-01-1-0447. Special thanks also are given to Joe Adario and Peter Kloumann of the X-ray Characterization Lab at MIT's Center for Materials Science and Engineering.

References

(1) POSS is a trademark of Hybrid Plastics (www.hybridplastics.com).

(2) Lichtenhan, J. D.; Vu, N. Q.; Carter, J. A.; Gilman, J. W.; Feher, F. J. *Macromolecules* **1993**, *26*, 2141.

(3) Schwab, J. J.; Lichtenhan, J. D. *Appl. Organomet. Chem.* **1998**, *12*, 707.

(4) Lucke, S.; Stoppek-Langner, K. *Appl. Surf. Sci.* **1999**, *145*, 713.

(5) Li, G. Z.; Wang, L. C.; Ni, H. L.; Pittman, C. U. *J. Inorg. Organomet. Polym.* **2001**, *11*, 123.

(6) Zheng, L.; Farris, R. J.; Coughlin, E. B. *Macromolecules* **2001**, *34*, 8034.

(7) Mather, P. T.; Jeon, H. G.; Romo-Uribe, A.; Haddad, T. S.; Lichtenhan, J. D. *Macromolecules* **1999**, *32*, 1194.

(8) Xu, H. Y.; Kuo, S. W.; Chang, F. C. *Polym. Bull.* **2002**, *48*, 469.

(9) Xu, H. Y.; Kuo, S. W.; Lee, J. S.; Chang, F. C. *Macromolecules* **2002**, *35*, 8788.

(10) Romo-Uribe, A.; Mather, P. T.; Haddad, T. S.; Lichtenhan, J. D. *J. Polym. Sci. B: Polym. Phys.* **1998**, *36*, 1857.

(11) Zhang, W. H.; Fu, B. X.; Seo, Y.; Schrag, E.; Hsiao, B.; Mather, P. T.; Yang, N. L.; Xu, D. Y.; Ade, H.; Rafailovich, M.; Sokolov, J. *Macromolecules* **2002**, *35*, 8029.

(12) Blanski, R. L.; Phillips, S. H.; Chaffee, K.; Lichtenhan, J.; Lee, A.; Geng, H. P. *Polymer Preprints* **2000**, *41*, 585.

(13) Zheng, L.; Waddon, A. J.; Farris, R. J.; Coughlin, E. B. *Macromolecules* **2002**, *35*, 2375.

(14) Vaia, R. A.; Giannelis, E. P. *MRS Bulletin* **2001**, *26*, 394.

(15) Fu, B. X.; Gelfar, M. Y.; Hsiao, B. S.; Phillips, S.; Viers, B.; Blanski, R.; Ruth, P *Polymer* **2003**, *44*, 1499.

(16) Zhang, Q.; Archer, L. A. *Langmuir* **2002**, *18*, 10435.

(17) Mackay, M. E.; Dao, T. T.; Tuteja, A.; Ho, D. L.; Van Horn, B.; Kim, H. C.; Hawker, C. J. *Nat. Mater.* **1996**, *2*, 762.

(18) Einstein, A. *Ann. Phys. (Leipz.)* **1906**, *19*, 371.

(19) (a) Brown Jr., J. F.; Vogt Jr., L. H. *J. Am. Chem. Soc.* **1965**, *87*, 4313. (b) Feher, F. J.; Newman, D. A.; Walzer, J. F. *J. Am. Chem. Soc.* **1989**, *111*, 1741. (c) Feher, F. J.; Budzichowski, T. A.; Blanski, R. L.; Weller, K. L.; Ziller, J. W. *Organometallics* **1991**, *10*, 2526. (c) Feher, F. J.; Terroba, R.; Ziller, J. W. *Chem. Commun.* **1999**, *22*, 2309.

(20) Barry, A. J.; Daudt, W. H.; Domicone, J. J.; Gilkey, J.W. *J. Am. Chem. Soc.* **1955**, *77*, 4248.

(21) Larsson, K. *Ark. Kemi* **1960**, *16*, 209.

(22) Wu, S. *J. Polym. Sci. B: Polym. Phys.* **1989**, *27*, 723.

(23) Lomellini, P.; Lavagnini, L. *Rheol. Acta* **1992**, *31*, 175.

(24) Larson, R. G. *The Structure and Rheology of Complex Fluids*; Oxford University Press: New York, 1998.

(25) Fuchs, K.; Friedrich, C.; Weese, J. *Macromolecules* **1996**, *29*, 5893.

(26) Dealy, J. M.; Wissbrun, K.F. *Melt Rheology and Its Role in Plastics Processing*; Von Nostrand Reinhold: New York, 1990.

(27) Smallwood, H. M. *J. Appl. Phys.* **1944**, *15*, 758.

(28) Poslinski, A. J.; Ryan, M. E.; Gupta, R. K.; Seshadri, S. G.; Frechette, F. J. *J. Rheol.* **1988**, *32*, 703.

(29) Friedrich, C.; Scheuchenpflug, W.; Neuhausler, S.; Rosch, J. *J. Appl. Polym. Sci.* **1995**, *57*, 499.

(30) Yurekli, K.; Krishnamoorti, R.; Tse, M. F.; McElrath, K. O.; Tsou, A. H.; Wang, H.-C. *J. Polym. Sci. B: Polym. Phys.* **2000**, *39*, 256.

(31) (a) Batchelor, G. K. *J. Fluid Mech.* **1970**, *41*, 545. (b) Batchelor, G. K. *J. Fluid Mech.* **1971**, *46*, 813. (c) Batchelor, G. K. *J. Fluid Mech.* **1977**, *83*, 97.

(32) Doi, M.; Edwards, S. F. *The Theory of Polymer Dynamics*; Clarendon Press: Oxford, 1986.

(33) Lim, Y. T.; Park, O. O. *Rheol. Acta* **2001**, *40*, 220.

(34) Ferry, J. D. *Viscoelastic Properties of Polymers*, 3rd. Ed.; John Wiley & Sons: New York, 1980.

(35) Fetters, L. J.; Graessley, W. W.; Kiss, A. D. *Macromolecules* **1991**, *11*, 3136.

(36) Doolittle, A. K.; Doolittle, D. B. *J. Appl. Phys.* **1957**, *28*, 901.

Tables

Table 1
Polymers Used in the Study

Polymer Name	POSS Type	POSS Content (Wt.%)	POSS Content (mol%)	M_w (g/mol)	PDI	x_w
HP	---	0	0	80200	1.68	802
HP_2	---	0	0	260000	1.89	2600
CP_{iBu15}	Isobutyl	15	2.1	205000	2.26	1742
$CP_{iBu25Hi}$	Isobutyl	25	3.4	560000	2.64	4351
CP_{iBu25}	Isobutyl	25	3.4	62700	1.73	487
CP_{Cp25}	Cyclopentyl	25	3.1	720000	3.21	5594

Table 2
Quantitative Melting Behavior of Octaisobutyl-POSS-filled PMMA

Blend	T_m^1 (^{0}C)	ΔH_1 (J/g,$_{POSS}$)	T_m^2 (^{0}C)	ΔH_2 (J/g,$_{POSS}$)	$\Delta H_1/\Delta H_1^*$	$\Delta H_2/\Delta H_2^*$
$2.5F_{iBu}$/97.5HP	51	1.34	---	0.00	0.11	0.00
$5F_{iBu}$/95HP	53	3.18	255	3.26	0.27	0.20
$10F_{iBu}$/90HP	54	4.90	263	11.4	0.42	0.71
$30F_{iBu}$/70HP	58	7.46	266	12.3	0.63	0.76
$100F_{iBu}$	60	11.8	261	16.1	1.00	1.00

Table 3
Rheological Properties of Unfilled, Entangled Polymers

Polymer	Wt.% POSS	G_N^0 (Pa)	M_e (g/mol)	Z (M_w/M_e)	T_g (C)
		(T_0 = 170^{0}C)			
HP_2	0	5.2×10^5	6200	43	124
CP_{iBu15}	15	4.5×10^5	7100	29	87
$CP_{iBu25Hi}$	25	3.4×10^5	9400	60	113
CP_{Cp25}	25	3.7×10^5	8900	81	126

Table 4						
WLF Parameters, Zero-Shear-Rate Viscosities and T_g values for						
Untethered-POSS-filled Homopolymer Blends						
Blend Composition	c_1^0	c_2^0 (K)	f_0/B	f_g/B	η_0 (Pa s)	T_g (^{0}C)
			(T_0 = 190^{0}C)	(T = T_g)	(T_0 = 190^{0}C)	
100HP	8.6	207	0.050	0.030	1.2 x 10^5	105
1F_{Cy}/99HP	8.7	208	0.050	0.030	9.6 x 10^4	105
3F_{Cy}/97HP	9.0	214	0.048	0.029	1.0 x 10^5	105
5F_{Cy}/95HP	9.0	213	0.048	0.029	1.1 x 10^5	106
10F_{Cy}/90HP	9.9	233	0.044	0.028	1.6 x 10^5	106
20F_{Cy}/80HP	7.6	176	0.057	0.030	*a*	105
30F_{Cy}/70HP[b]	5.9	154	0.074	0.033	*d*	106
2.5F_{iBu}/97.5HP	8.4	202	0.052	0.030	9.1 x 10^4	105
5F_{iBu}/95HP	8.6	205	0.051	0.030	9.2 x 10^4	105
10F_{iBu}/90HP	9.4	212	0.047	0.027	1.2 x 10^5	103
20F_{iBu}/80HP	7.4	175	0.059	0.030	*c*	105
30F_{iBu}/70HP	8.0	189	0.054	0.030	*d*	106
a > 1.8 x 10^5 Pa s						
b WLF fit was poor and the coefficients are considered unreliable						
c > 1.9 x 10^5 Pa s						
d Sample exhibited a yield stress						

Table 5							
WLF Parameters, Zero-Shear-Rate Viscosities and T_g values for							
Untethered-POSS-filled Copolymer Blends							
Blend Composition	c_1^0	c_2^0 (K)	f_0/B	f_g/B	η_0 (Pa s)	T_g (^{0}C)	$N_{Untethered}$ /
			(T_0 = 135^{0}C)		(T_0 = 150^{0}C)		$N_{\text{Tethered POSS}}$
100CP_{iBu25}	9.1	120	0.048	0.032	4.3 x 10^5	95	0.00
2F_{iBu}/98CP_{iBu25}	6.6	90	0.066	0.037	5.0 x 10^5	96	0.09
5F_{iBu}/95CP_{iBu25}	6.6	85	0.065	0.035	6.8 x 10^5	95	0.23
20F_{iBu}/80CP_{iBu25}	8.3	110	0.053	0.033	1.8 x 10^6	95	1.08
30F_{iBu}/70CP_{iBu25}[a]	12.5	176	0.035	0.028	*b*	103	1.85
[a] WLF fit was poor and the coefficients are considered unreliable							
[b] > 5.0 x 10^6 Pa s							

Figure 1. Three component composition diagram for untethered-POSS filler (F), tethered-POSS containing copolymer with PMMA backbone (CP), and PMMA homopolymer (HP). The arrows represent the ranges of composition analyzed in the present study.

Figure 2. WAXD patterns for blends composed of: (a) cyclohexyl-POSS in PMMA homopolymer; (b) isobutyl-POSS in copolymer containing 25 wt% isobutyl-POSS on the chain (CP_{iBu25}).

Figure 3. WAXD patterns for isobutyl-POSS powder both below the first melting transition of the powder (30°C) and above (110°C), showing the absence of certain prominent peaks at the higher temperature.

Figure 4. DSC curves for PMMA homopolymer filled with isobutyl-POSS. Two distinct melting transitions are apparent in the more highly-filled samples, with the size of the endotherms proportionally larger at higher loadings.

Figure 5. Heats of fusion per gram isobutyl-POSS in the sample for both melting transitions of isobutyl-POSS-filled-PMMA blends.

Figure 6. Master curves for the (a) storage modulus G' and the (b) loss modulus G'' for entangled copolymers containing varied amounts of tethered-POSS on a PMMA backbone. Master curves for an entangled PMMA homopolymer are also shown. (T_0 = 170°C)

Figure 7. Master curves for the (a) storage modulus and the (b) loss modulus for blends of isobutyl-POSS between 0 and 30 vol% in a copolymer containing 25 wt% isobutyl-POSS on the chain (CP_{iBu25}). (T_0 = 150°C)

Figure 8. Master curves for the storage and loss moduli of three different samples: PMMA homopolymer, PMMA homopolymer containing 5 vol% cyclohexyl-POSS, and PMMA homopolymer containing 5 vol% isobutyl-POSS. (T_0 = 190°C)

Figure 9. Master curves for the storage modulus of PMMA filled with between 0 and 30 vol% with cyclohexyl-POSS. (T_0 = 190°C)

Figure 10. Plateau moduli for blends containing untethered-POSS, $G_N^0(\phi)$, normalized by the respective unfilled polymer plateau modulus, $G_N^0(0)$. Data are plotted for PMMA homopolymer filled with both cyclohexyl-POSS and isobutyl-POSS and for isobutyl-POSS-filled in a copolymer containing 25 wt% isobutyl-POSS on the chain (CP_{iBu25}). The lines are fits to the Guth-Smallwood Equaton (Eq. 5).

Figure 11. Zero-shear-rate viscosities for blends containing untethered-POSS, $\eta_0(\phi)$, normalized by the respective unfilled polymer plateau modulus, $\eta_0(0)$. Data are plotted for PMMA homopolymer filled with both cyclohexyl- and isobutyl-POSS and for isobutyl-POSS-filled in copolymer containing 25 wt% isobutyl-POSS on the chain (CP_{iBu25}). The dotted line represents the prediction of the Einstein-Batchelor Equation (Eq. 7), while the dashed line is a plot of Eq. 7 for an effective volume fraction 2.75 times that of the actual filler value.

Figure 12. Horizontal and vertical concentration shift factors for the three blend systems obtained by shifting the storage modulus curves for each blend sample onto the respective unfilled polymer's master curve.

Figure 13. Schematic of POSS-polymer blends in the (a) filler-homopolymer system (F/HP) and the (b) filler copolymer system (F/CP). In the F/HP case, untethered-POSS does not interact strongly with the PMMA matrix and thus can only plasticize the matrix in a nanodispersed state or reinforce the matrix by forming crystallites. In the F/CP case, the untethered-POSS and tethered-POSS on the copolymer chain associate into nanoscopic domains (indicated by boxes) which retard chain relaxation processes in the melt.

Figure 14. Loss tangent (G''/G') curves for PMMA filled with 10 vol% cyclohexyl-POSS: (a) individual temperatures unshifted; (b) all curves shifted to reference temperature T_0 = 190°C.

Figure 14. WLF plots for: (a) PMMA homopolymer and homopolymer containing 10 vol% cyclohexyl-POSS (T_0 = 190°C); (b) copolymer containing 25 wt% isobutyl-POSS on the chain and respective copolymer containing 5 vol% isobutyl-POSS (T_0 = 135°C).

Fig. 1

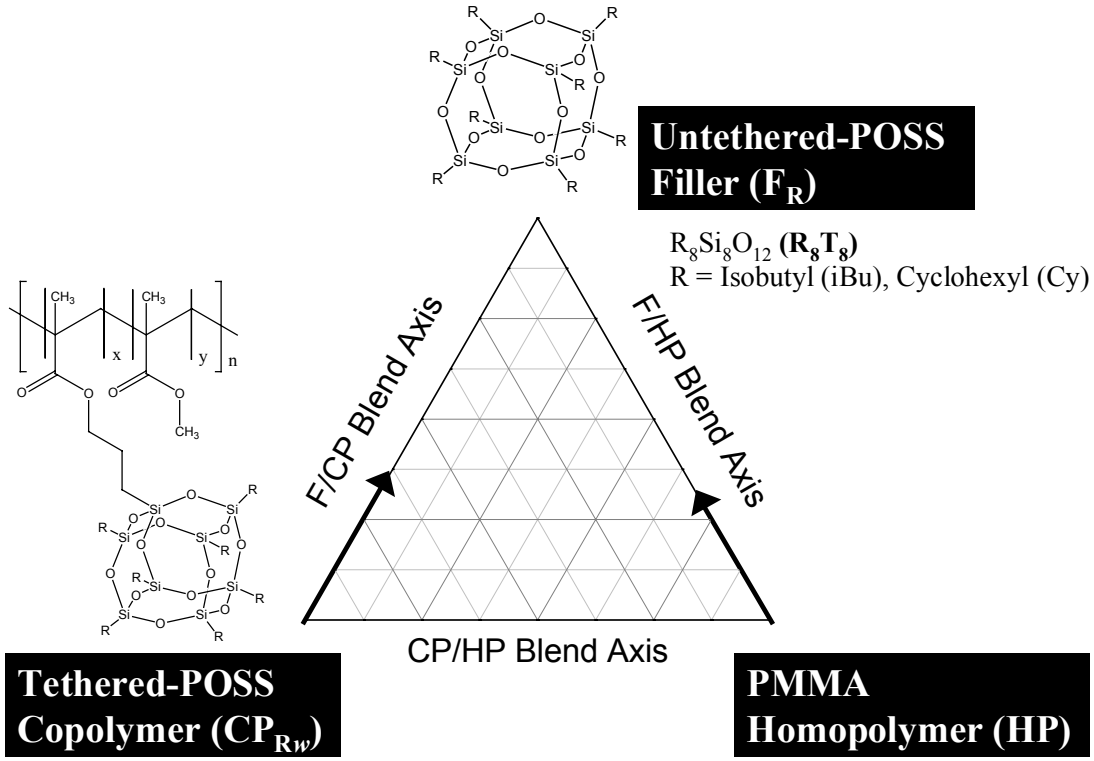
Untethered-POSS Filler (F_R)
$R_8Si_8O_{12}$ (R_8T_8)
R = Isobutyl (iBu), Cyclohexyl (Cy)
F/CP Blend Axis
F/HP Blend Axis
CP/HP Blend Axis
Tethered-POSS Copolymer (CP_{Rw})
R = Isobutyl, Cyclopentyl (Cp)
PMMA Homopolymer (HP)

Fig. 2

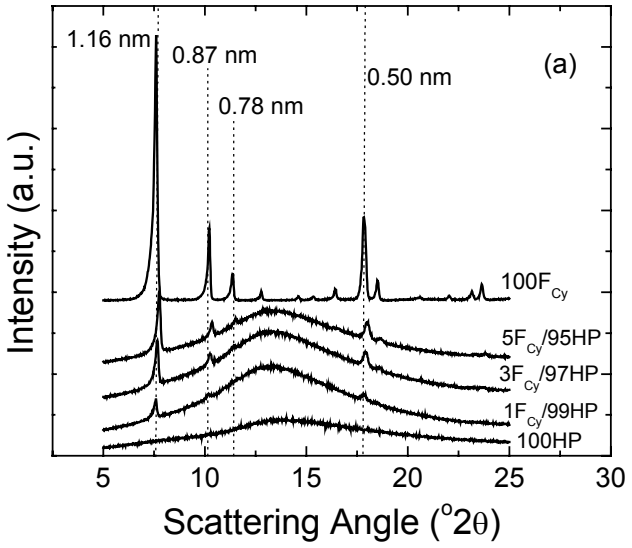
1.16 nm
0.87 nm
0.78 nm
0.50 nm
(a)
100F$_{Cy}$
5F$_{Cy}$/95HP
3F$_{Cy}$/97HP
1F$_{Cy}$/99HP
100HP
Intensity (a.u.)
Scattering Angle (^{o}2θ)

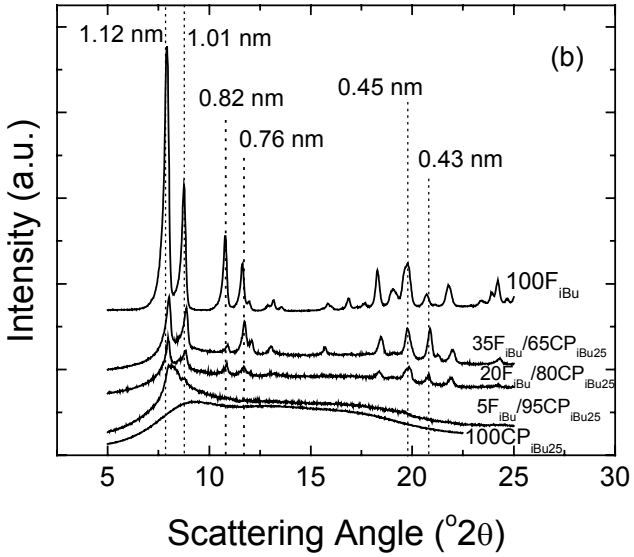
1.12 nm
1.01 nm
0.82 nm
0.76 nm
0.45 nm
0.43 nm
(b)
100F$_{iBu}$
35F$_{iBu}$/65CP$_{iBu25}$
20F$_{iBu}$/80CP$_{iBu25}$
5F$_{iBu}$/95CP$_{iBu25}$
100CP$_{iBu25}$
Intensity (a.u.)
Scattering Angle (^{o}2θ)

Fig. 3

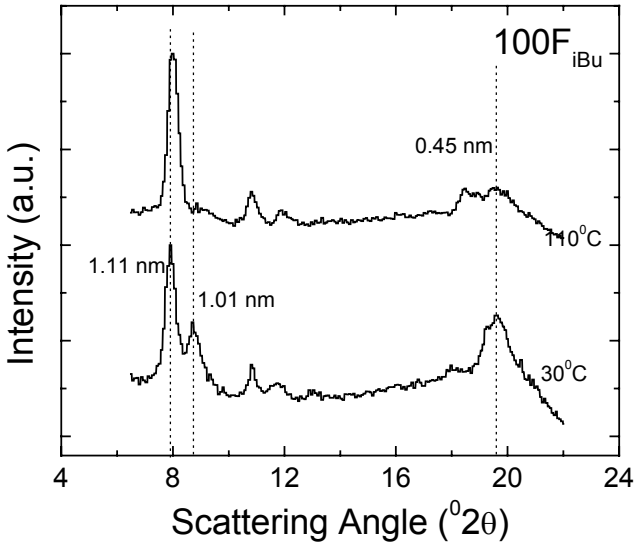
100F$_{iBu}$
0.45 nm
110^{0}C
1.11 nm
1.01 nm
30^{0}C
Intensity (a.u.)
4
8
12
16
20
24
Scattering Angle (^{0}2θ)

Fig. 4

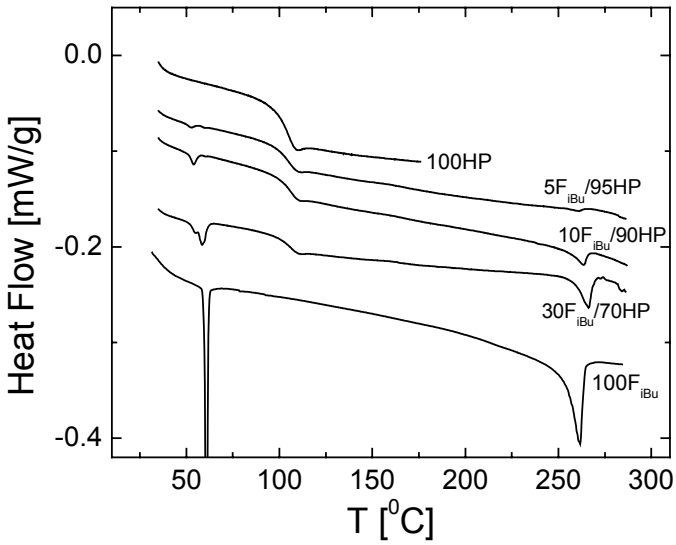
0.0
-0.2
-0.4
Heat Flow [mW/g]
50
100
150
200
250
300
T [^{0}C]
100HP
5F$_{iBu}$/95HP
10F$_{iBu}$/90HP
30F$_{iBu}$/70HP
100F$_{iBu}$

Fig. 5

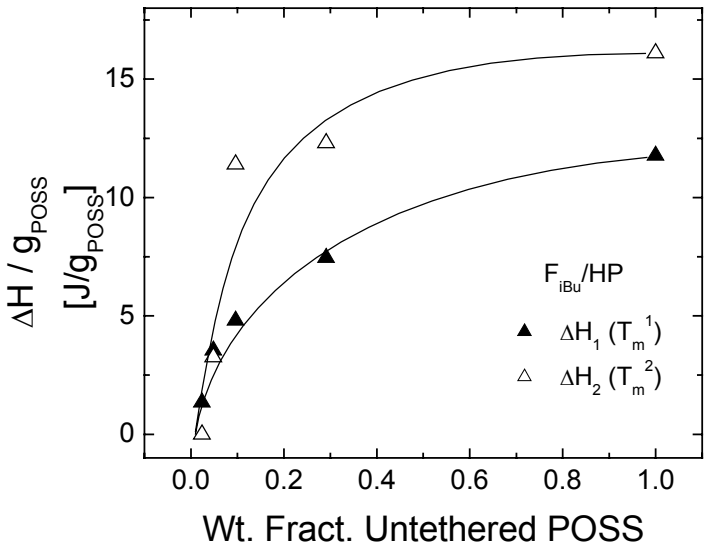
ΔH / g_POSS [J/g_POSS]
15
10
5
0
0.0
0.2
0.4
0.6
0.8
1.0
Wt. Fract. Untethered POSS
F_iBu/HP
ΔH_1 (T_m^1)
ΔH_2 (T_m^2)

Fig. 6

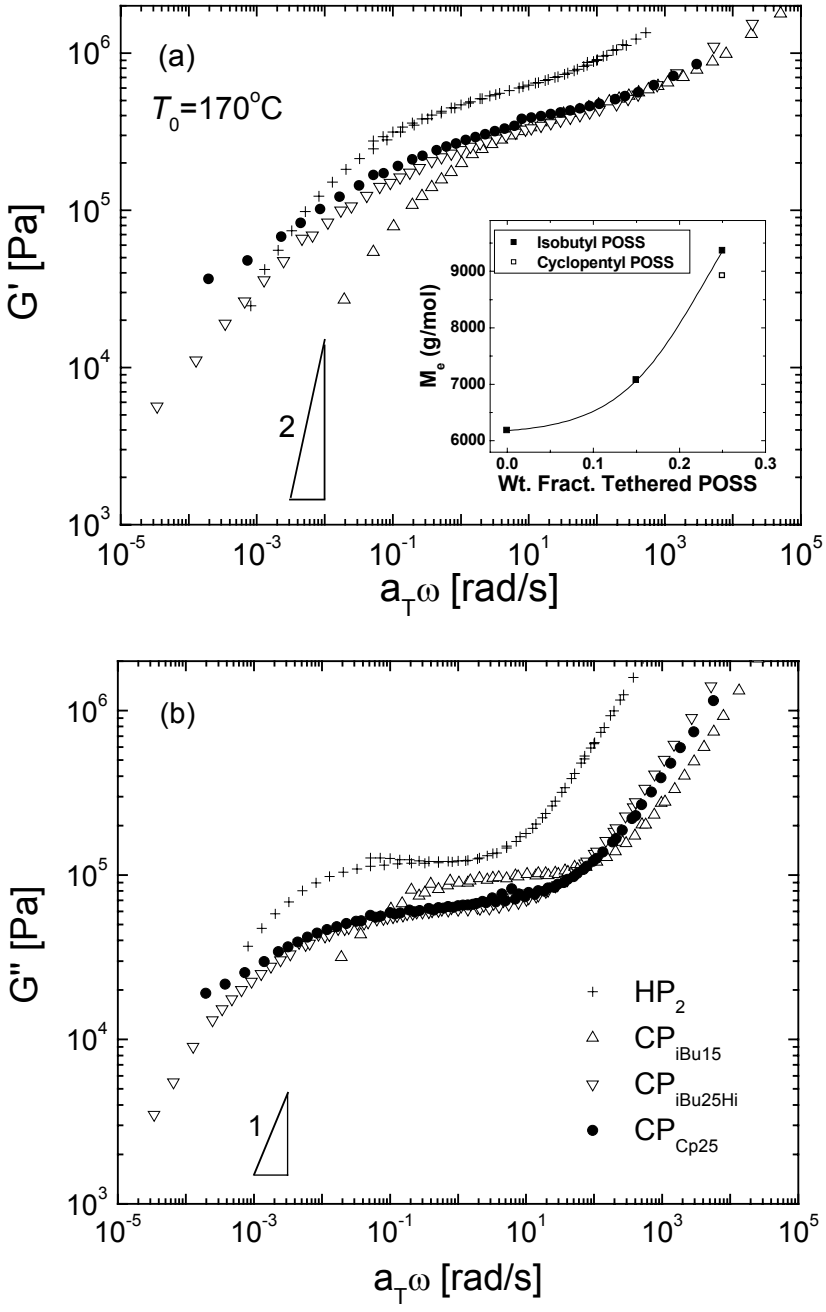
(a)
T_0=170°C
G' [Pa]
$a_T\omega$ [rad/s]
2
Isobutyl POSS
Cyclopentyl POSS
M_e (g/mol)
Wt. Fract. Tethered POSS
(b)
G'' [Pa]
$a_T\omega$ [rad/s]
1
HP_2
CP_{iBu15}
$CP_{iBu25Hi}$
CP_{Cp25}

Fig. 7

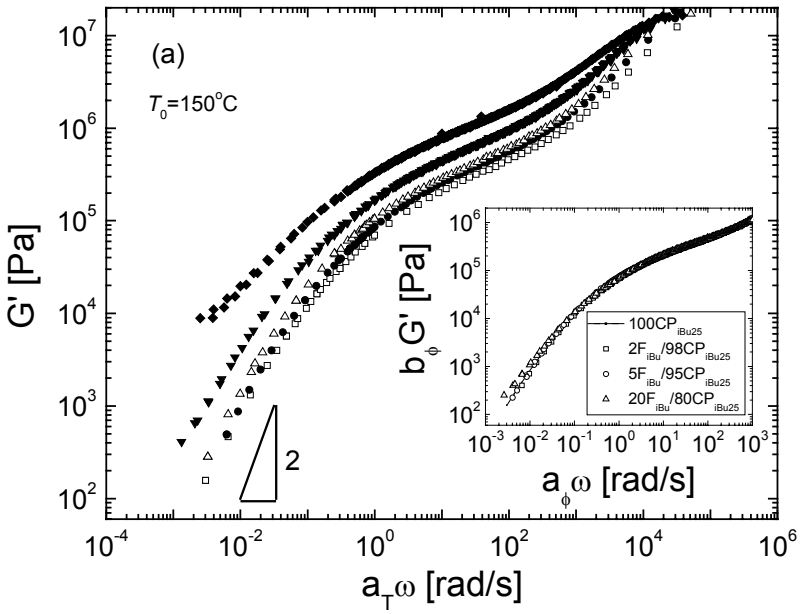
(a)
T_0=150°C
G' [Pa]
$a_T\omega$ [rad/s]
2
b_ϕG' [Pa]
$a_\phi\omega$ [rad/s]
100CP$_{iBu25}$
2F$_{iBu}$/98CP$_{iBu25}$
5F$_{iBu}$/95CP$_{iBu25}$
20F$_{iBu}$/80CP$_{iBu25}$

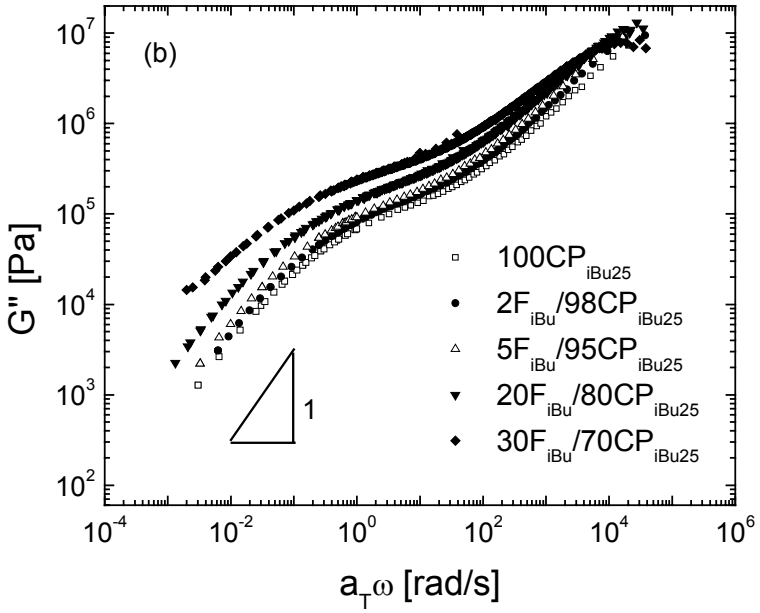
(b)
G'' [Pa]
$a_T\omega$ [rad/s]
1
100CP$_{iBu25}$
2F$_{iBu}$/98CP$_{iBu25}$
5F$_{iBu}$/95CP$_{iBu25}$
20F$_{iBu}$/80CP$_{iBu25}$
30F$_{iBu}$/70CP$_{iBu25}$

Fig. 8

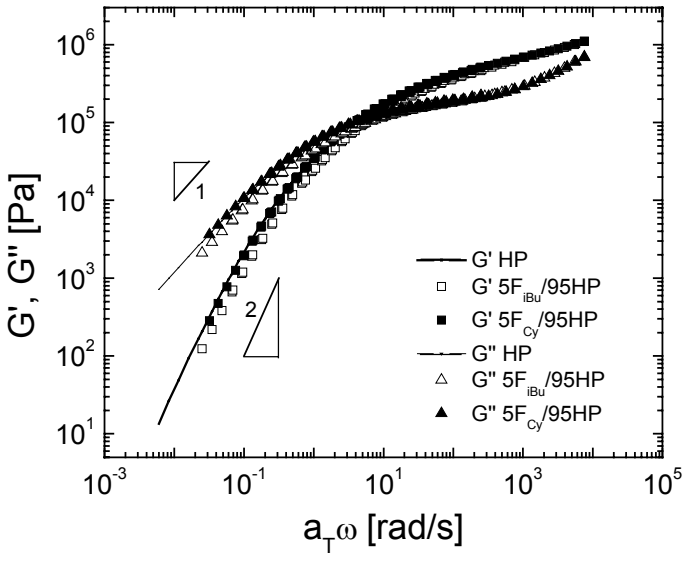
G', G'' [Pa]
$a_T\omega$ [rad/s]
1
2
G' HP
G' 5F$_{iBu}$/95HP
G' 5F$_{Cy}$/95HP
G'' HP
G'' 5F$_{iBu}$/95HP
G'' 5F$_{Cy}$/95HP

Fig. 9

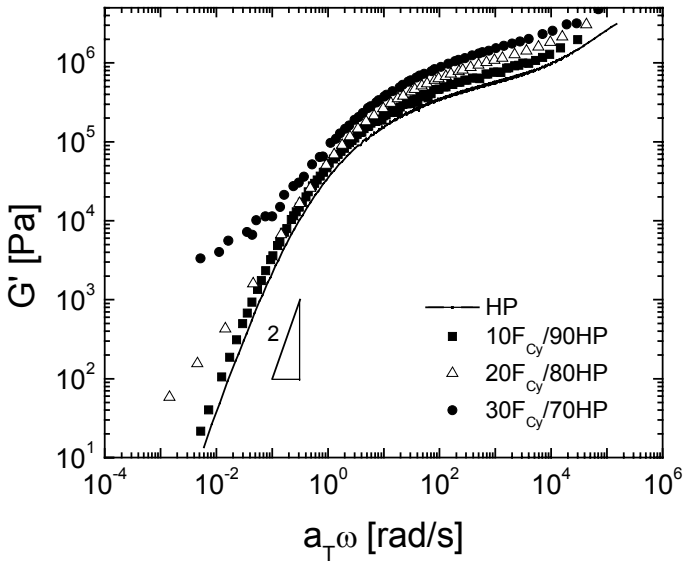

Fig. 10

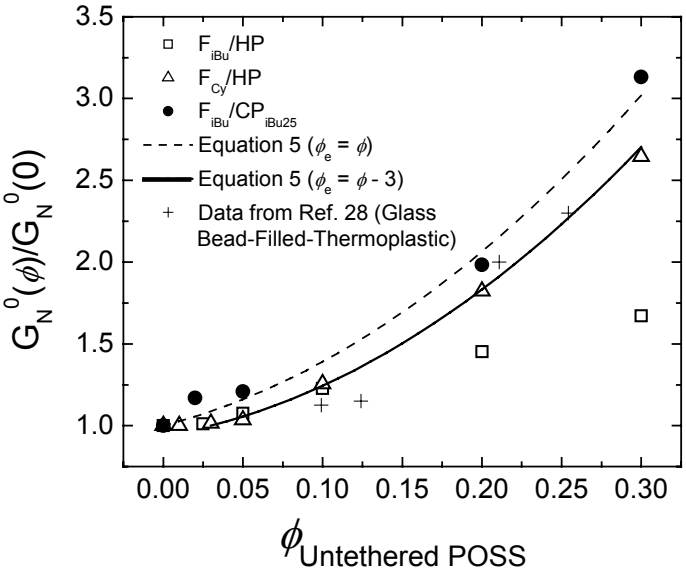
3.5
3.0
2.5
2.0
1.5
1.0
0.00
0.05
0.10
0.15
0.20
0.25
0.30
$G_N^0(\phi)/G_N^0(0)$
$\phi_{Untethered\ POSS}$
F_{iBu}/HP
F_{Cy}/HP
F_{iBu}/CP_{iBu25}
Equation 5 ($\phi_e = \phi$)
Equation 5 ($\phi_e = \phi - 3$)
Data from Ref. 28 (Glass Bead-Filled-Thermoplastic)

Fig. 11

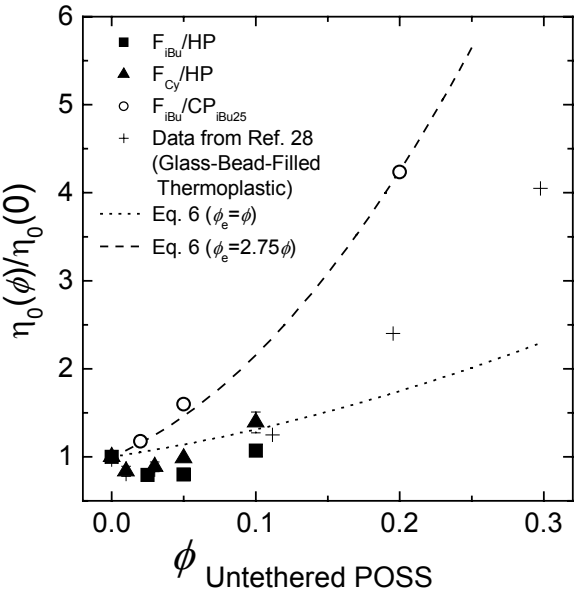
F_{iBu}/HP
F_{Cy}/HP
F_{iBu}/CP_{iBu25}
Data from Ref. 28
(Glass-Bead-Filled
Thermoplastic)
Eq. 6 ($\phi_e=\phi$)
Eq. 6 ($\phi_e=2.75\phi$)
$\eta_0(\phi)/\eta_0(0)$
ϕ Untethered POSS
0.0
0.1
0.2
0.3
1
2
3
4
5
6

Fig. 12 (a), (b)

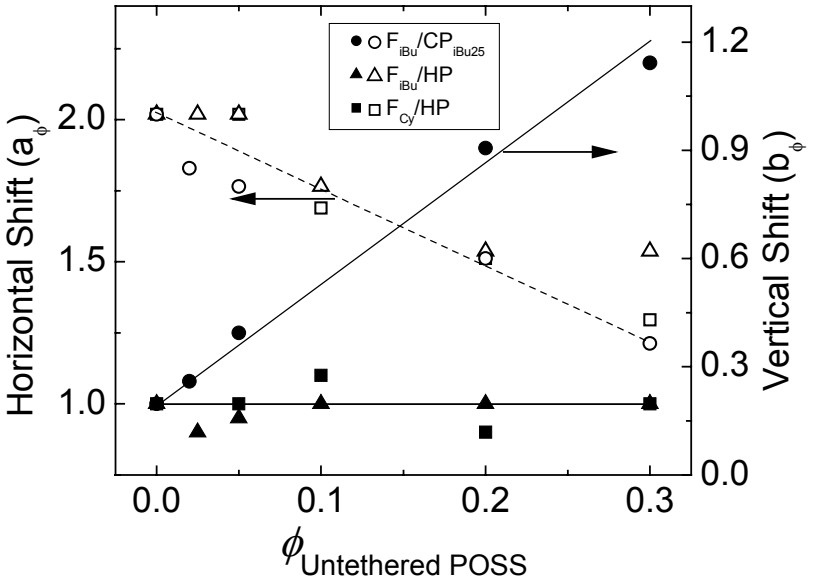
F_iBu/CP_iBu25
F_iBu/HP
F_Cy/HP
Horizontal Shift (a_φ)
Vertical Shift (b_φ)
2.0
1.5
1.0
1.2
0.9
0.6
0.3
0.0
0.0
0.1
0.2
0.3
φ Untethered POSS

Fig. 13(a), (b)

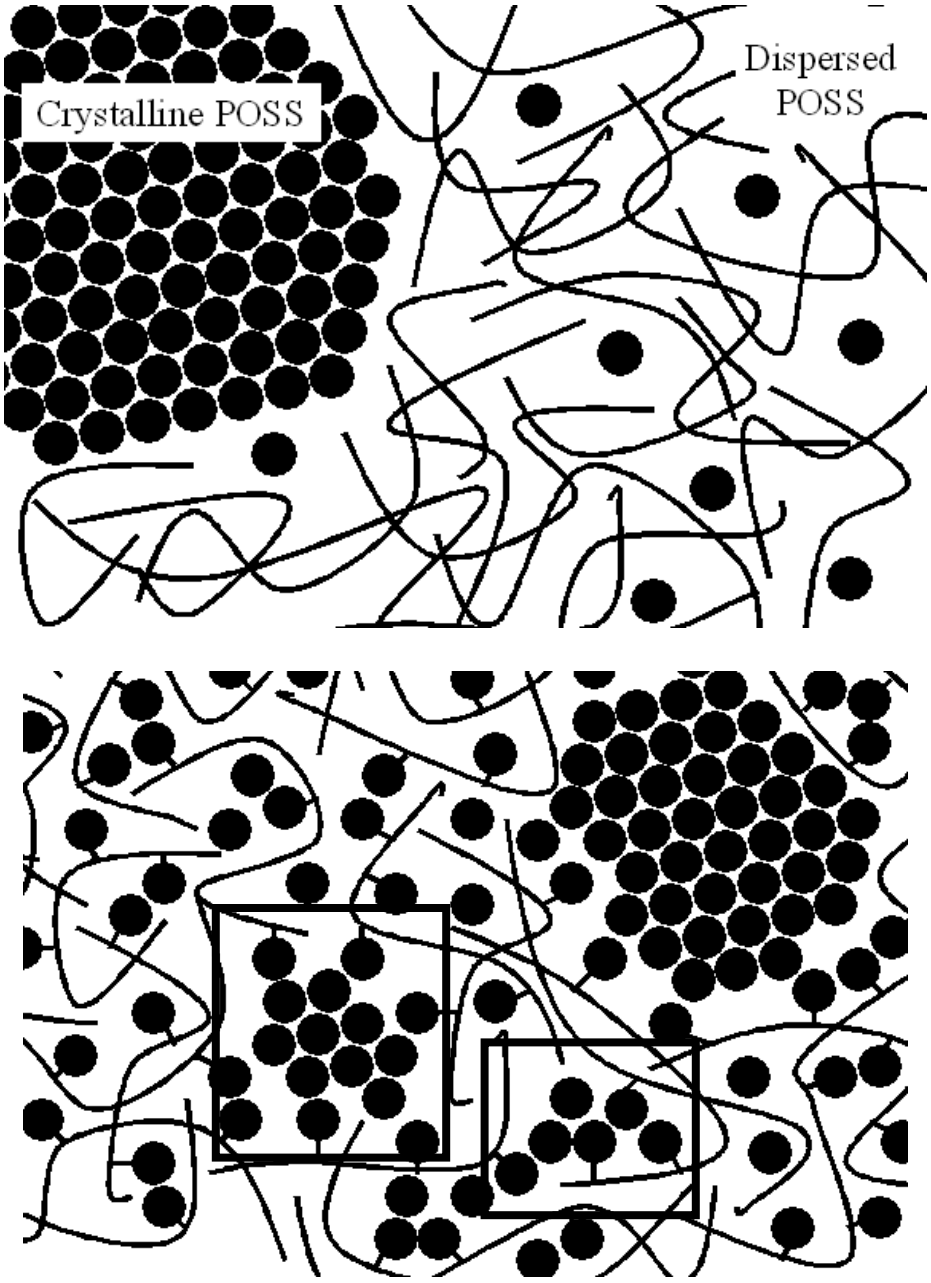

Fig. 14

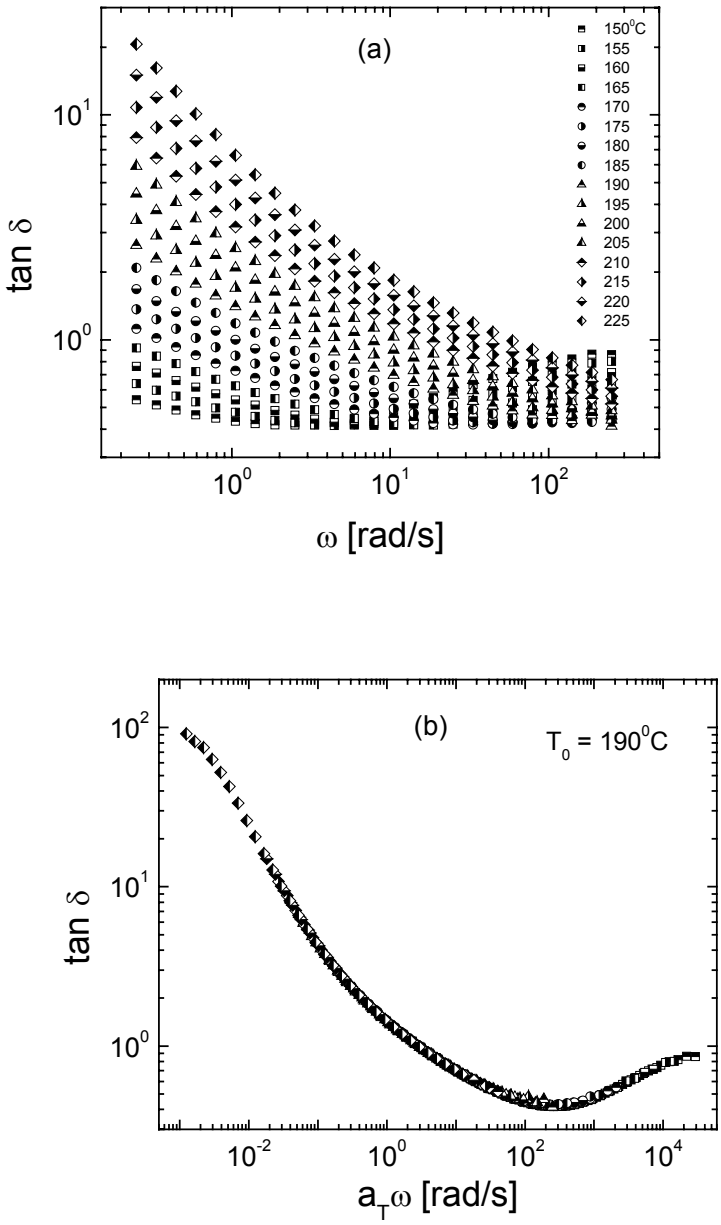
(a)
150°C
155
160
165
170
175
180
185
190
195
200
205
210
215
220
225
tan δ
ω [rad/s]
(b)
T0 = 190°C
tan δ
aTω [rad/s]

Fig. 15

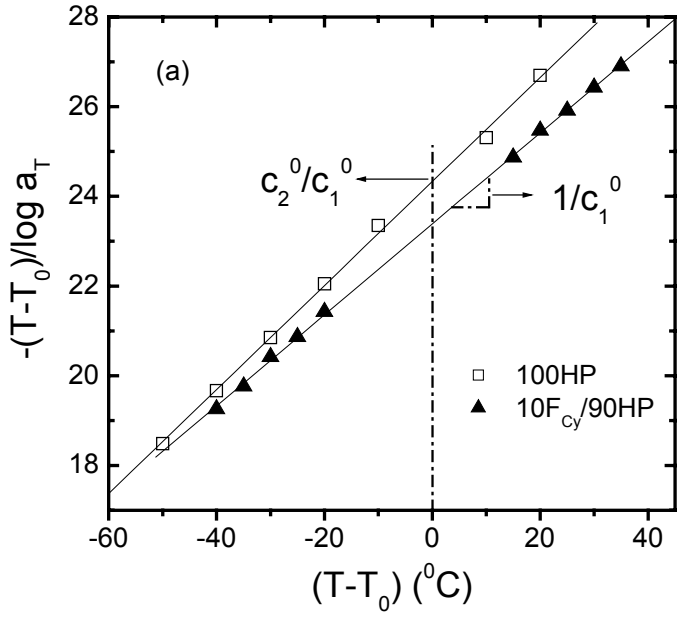
(a)
c_2^0/c_1^0
$1/c_1^0$
100HP
10F$_{Cy}$/90HP
-(T-T$_0$)/log a$_T$
(T-T$_0$) (^{0}C)

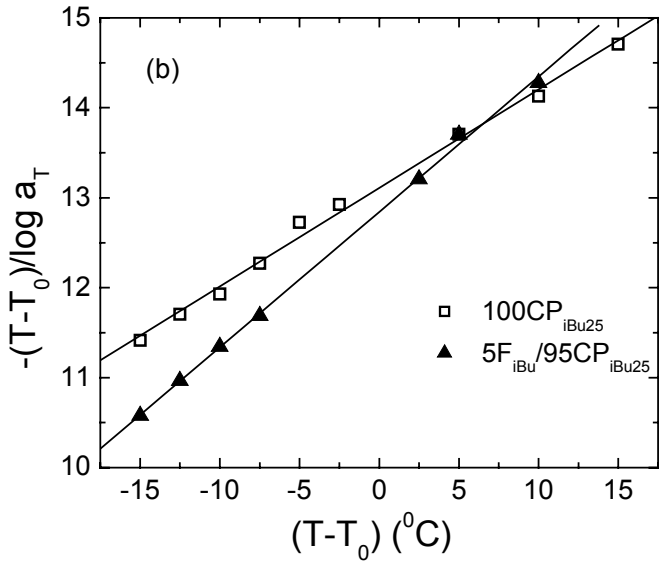
(b)
100CP$_{iBu25}$
5F$_{iBu}$/95CP$_{iBu25}$
-(T-T$_0$)/log a$_T$
(T-T$_0$) (^{0}C)